

Deletion of *nfnAB* in *Thermoanaerobacterium saccharolyticum* and Its Effect on Metabolism

Jonathan Lo,^{a,e} Tianyong Zheng,^{a,e} Daniel G. Olson,^{b,e} Natalie Ruppertsberger,^{b,e} Shital A. Tripathi,^c Adam M. Guss,^{d,e} Lee R. Lynd^{a,b,d,e}

Department of Biological Sciences, Dartmouth College, Hanover, New Hampshire, USA^a; Thayer School of Engineering, Dartmouth College, Hanover, New Hampshire, USA^b; Total New Energies USA, Inc., Emeryville, California, USA^c; Biosciences Division, Oak Ridge National Laboratory, Oak Ridge, Tennessee, USA^d; BioEnergy Science Center, Oak Ridge, Tennessee, USA^e

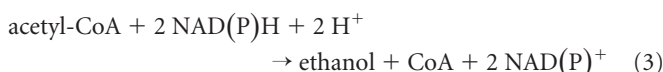
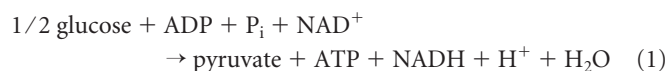
ABSTRACT

NfnAB catalyzes the reversible transfer of electrons from reduced ferredoxin and NADH to 2 NADP⁺. The NfnAB complex has been hypothesized to be the main enzyme for ferredoxin oxidization in strains of *Thermoanaerobacterium saccharolyticum* engineered for increased ethanol production. NfnAB complex activity was detectable in crude cell extracts of *T. saccharolyticum*. Activity was also detected using activity staining of native PAGE gels. The *nfnAB* gene was deleted in different strains of *T. saccharolyticum* to determine its effect on end product formation. In wild-type *T. saccharolyticum*, deletion of *nfnAB* resulted in a 46% increase in H₂ formation but otherwise little change in other fermentation products. In two engineered strains with 80% theoretical ethanol yield, loss of *nfnAB* caused two different responses: in one strain, ethanol yield decreased to about 30% of the theoretical value, while another strain had no change in ethanol yield. Biochemical analysis of cell extracts showed that the Δ *nfnAB* strain with decreased ethanol yield had NADPH-linked alcohol dehydrogenase (ADH) activity, while the Δ *nfnAB* strain with unchanged ethanol yield had NADH-linked ADH activity. Deletion of *nfnAB* caused loss of NADPH-linked ferredoxin oxidoreductase activity in all cell extracts. Significant NADH-linked ferredoxin oxidoreductase activity was seen in all cell extracts, including those that had lost *nfnAB*. This suggests that there is an unidentified NADH:ferredoxin oxidoreductase (distinct from *nfnAB*) playing a role in ethanol formation. The NfnAB complex plays a key role in generating NADPH in a strain that had become reliant on NADPH-ADH activity.

IMPORTANCE

Thermophilic anaerobes that can convert biomass-derived sugars into ethanol have been investigated as candidates for biofuel formation. Many anaerobes have been genetically engineered to increase biofuel formation; however, key aspects of metabolism remain unknown and poorly understood. One example is the mechanism for ferredoxin oxidation and transfer of electrons to NAD(P)⁺. The electron-bifurcating enzyme complex NfnAB is known to catalyze the reversible transfer of electrons from reduced ferredoxin and NADH to 2 NADP⁺ and is thought to play key roles linking NAD(P)(H) metabolism with ferredoxin metabolism. We report the first deletion of *nfnAB* and demonstrate a role for NfnAB in metabolism and ethanol formation in *Thermoanaerobacterium saccharolyticum* and show that this may be an important feature among other thermophilic ethanologenic anaerobes.

Plant biomass is a sustainable and low-carbon source for biofuels; however, its recalcitrance makes conversion into fuels difficult (1). One of the leading strategies for low-cost conversion of plant biomass into fuels is consolidated bioprocessing (CBP), wherein one or more microbes solubilize plant cell walls and ferment the resulting sugars into fuel without exogenously added enzymes. The thermophilic anaerobe *Thermoanaerobacterium saccharolyticum* solubilizes components of plant biomass and produces ethanol as a fermentation product and thus is of interest for CBP (2). *T. saccharolyticum* has been engineered to make ethanol from sugars in amounts near 90% of the theoretical yield (3). This ethanologen strain of *T. saccharolyticum* was created by deleting lactate dehydrogenase (*ldh*), phosphotransacetylase (*pta*), and acetate kinase (*ack*). In *T. saccharolyticum*, glycolysis, pyruvate oxidation, and ethanol formation are believed to proceed by reactions 1, 2, and 3, respectively (4, 5) (where Fd_{ox} is oxidized ferredoxin, Fd_{red} is reduced ferredoxin, and acetyl-CoA is acetyl coenzyme A):



Reducing equivalents formed from reactions 1 and 2 are expected to be directed to ethanol formation via acetaldehyde and alcohol dehydrogenases (ADHs) (reaction 3). Use of only the re-

Received 14 May 2015 Accepted 23 June 2015

Accepted manuscript posted online 29 June 2015

Citation Lo J, Zheng T, Olson DG, Ruppertsberger N, Tripathi SA, Guss AM, Lynd LR. 2015. Deletion of *nfnAB* in *Thermoanaerobacterium saccharolyticum* and its effect on metabolism. *J Bacteriol* 197:2920–2929. doi:10.1128/JB.00347-15.

Editor: T. J. Silhavy

Address correspondence to Lee R. Lynd, Lee.R.Lynd@Dartmouth.edu.

Copyright © 2015, American Society for Microbiology. All Rights Reserved.

doi:10.1128/JB.00347-15

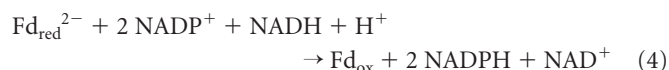
TABLE 1 Strains and plasmids used in this study

Strain or plasmid	Description	Reference or source
Strains		
<i>T. saccharolyticum</i> strains		
JW/SL-YS485	Wild type	Gift from Juergen Wiegel
LL1144	JW/SL-YS485 $\Delta nfnAB::Kan^r$	This work
M0353	$\Delta pta \Delta ack \Delta ldh \Delta pyrF$ (LL1174) ^a	17
LL1145	M0353 $\Delta nfnAB::Kan^r$	This work
M1442	$\Delta pta \Delta ack \Delta ldh adhE^{G544D}$ (LL1049) ^a	18
LL1220	M1442 $\Delta nfnAB::Kan^r$	This work
LL1222	LL1220 $\Delta xynA::nfnAB Ery^r$	This work
<i>E. coli</i> strains		
T7 Express lysY/l ^q	Used for heterologous protein expression	New England Biolabs
DH5 α	Used for plasmid screening and propagation	New England Biolabs
Plasmids		
pMU804	Disrupts <i>nfnAB</i> with kanamycin resistance gene	This work
pJLO30	pEXP5-NT TOPO expressing <i>T. saccharolyticum nfnAB</i>	This work
pJLO31	Inserts <i>nfnAB</i> with erythromycin resistance gene in <i>xynA</i> region	This work

^a Alternate strain name is given in parentheses.

ducing power from reaction 1 (i.e., NADH) would allow only 50% of the pyruvate generated by that reaction on a molar basis to be converted to ethanol. Increasing ethanol yield beyond 50% requires the use of the reducing equivalents generated by reaction 2 (i.e., Fd_{red}^{2-}). Since yields of ethanol exceed 50% in *T. saccharolyticum* strains, electrons from reduced ferredoxin (Fd_{red}) must be used for ethanol formation, assuming that glucose conversion to ethanol proceeds via reactions 1 to 3. Benzyl viologen (BV) reduction with NAD(P)H, an enzyme assay for electron transfer between NAD(P)(H) and ferredoxin, has been previously observed in *T. saccharolyticum* (3, 4) and was hypothesized to be encoded by Tsac_2085-Tsac_2086 (4). However, the observed activities were not directly attributed these genes, and the role of Tsac_2085-Tsac_2086 in ethanol formation was never conclusively demonstrated.

The NfnAB complex is an enzyme originally isolated from *Clostridium kluyveri* that contains two subunits (A and B) which together catalyze the oxidation of NADH and ferredoxin with the reduction of 2 NADP⁺ (reaction 4), known as NADH-dependent reduced ferredoxin: NADP⁺ oxidoreductase (NFN) activity (6). Although the reaction is reversible, the NfnAB complex likely catalyzes NADPH production *in vivo* (6, 7):



Ferredoxin:NAD(P)H oxidoreductase (FNOR) activity, measured by NADPH:BV reduction, was observed to increase in a *T. saccharolyticum* strain engineered for increased ethanol yield (3). NADPH:BV reduction can be catalyzed by the NfnAB complex, suggesting that it may be important for ethanol formation in this engineered strain. *T. saccharolyticum* appears to have an *nfnAB* homolog (Tsac_2085-Tsac_2086 has >60% amino acid identity to *C. kluyveri nfnAB*). The NfnAB complex could provide a key reaction for the formation of ethanol at high yield as it provides a mechanism for electron transfer from ferredoxin to NAD(P)⁺.

In this work, we attempt to answer the following questions about NfnAB. (i) What is the physiological role of the NfnAB

complex in *T. saccharolyticum*? (ii) Does this role change in strains that have been engineered for high-yield ethanol production?

To answer these questions, we utilized targeted gene deletion, heterologous gene expression, biochemical assays, and fermentation product analysis to understand the role of the NfnAB complex in anaerobic saccharolytic metabolism of *T. saccharolyticum*.

MATERIALS AND METHODS

Chemicals, strains, and molecular techniques. All chemicals were of molecular grade and obtained from Sigma-Aldrich (St. Louis, MO) or Fisher Scientific (Pittsburgh, PA) unless otherwise noted. A complete list of strains and plasmids is given in Table 1. *T. saccharolyticum* strain JW/SL-YS485 was kindly provided by Juergen Wiegel. *T. saccharolyticum* strain M0353 was a gift of the Mascoma Corporation (Lebanon, NH). Primers used for construction of plasmids and confirmation of *nfnAB* manipulations are listed in Table 2. Transformation and deletion of *nfnAB* in *T. saccharolyticum* (Tsac_2085-Tsac_2086) was accomplished with plasmid pMU804 (3). Plasmid pMU804 was generated by digesting plasmid pMU110 (8) with BamHI and XhoI (New England Biolabs, Beverly, MA) and using primers to amplify ~800 bp of regions flanking Tsac_2085-Tsac_2086 as well as a Kan^r gene. The resulting PCR products and plasmid digest were ligated together using yeast gap repair (9). Plasmids were extracted from *Saccharomyces cerevisiae* and transformed into *Escherichia coli* and screened for the correct insert by restriction digest (9). For complementation of *nfnAB* under the control of a xylose-inducible system into strain LL1220, ~500 bp of the *xynA* upstream region, *nfnAB*, an Erm^r gene, and ~500 bp of the downstream region of *xynA* were ligated together in that order using overlapping primers and Gibson assembly (New England Biolabs). The resulting fragment was cloned into a pCR-Blunt II vector (Life Technologies, Carlsbad, CA) for ease of propagation. The resulting plasmid was named pJLO31.

Media and growth conditions. All strains were grown anaerobically at 55°C, with an initial pH of 6.3. Bacteria for transformations and biochemical characterization were grown in modified DSMZ M122 rich medium containing 5 g/liter cellobiose and 4.5 g/liter yeast extract as previously described (10). To prepare cell extracts, cells were grown to an optical density at 600 nm (OD₆₀₀) of 0.5 to 0.8, separated from the medium by centrifugation, and used immediately or stored anaerobically in serum vials at -80°C as previously described (4, 5). For quantification of fermentation products on cellobiose, strains were grown with shaking in

TABLE 2 Primers used in this study

Primer	Sequence	Purpose
T.sac.nfnAB.ext.F	TGGCTTTTGTAGTGTGGGGT	Amplify <i>T. saccharolyticum</i> nfnAB external genomic fragment
T.sac.nfnAB.ext.R	CATTGTCATATCCCCCTTTT	
T.sacc.nfnAB.CDS.F	ATGAACGAGATTTTAGAGAAGAAGC	Amplify <i>T. saccharolyticum</i> nfnAB internal fragment
T.sac.nfnAB.int.R	GAGTGGGACTGTTAGGGA	
T.sacc.nfnAB.CDS.F	ATGAACGAGATTTTAGAGAAGAAGC	Clone coding sequence of <i>T. saccharolyticum</i> nfnAB for expression in <i>E. coli</i>
T.sacc.nfnAB.CDS.stop.R X03975	TCACTTTTCGCTTAAATATTTGTGTATAGAAGCTGCAGC ACCATTATTATCATGACATTAACCTATAAAAAAGGCCTGC AAGCACACAGCTTATGC	Clone <i>T. saccharolyticum</i> nfnAB 3' flank for deletion plasmid pMU804
X03976	CCTCCAATAACTACGTGGTCTTGAGGAAATACACCACGC	
X03977	GCGTGGTGTATTTCCTCAAGACCACGTAGTTATTGGGAGG	Clone Kan ^r insertion cassette for plasmid pMU804
X03978	CTTGAGGTGTGAAAGCAATGAGAGTGCATACAAATTCCTCG	
X03979	CGAGGAATTTGTATCGACTCTCATTGCTTTCACACCTCCAAG	Clone <i>T. saccharolyticum</i> nfnAB 5' flank for deletion plasmid pMU804
X03980	GGAATTGTGAGCGGATAACAATTTACACAGGAAACAGCTTG CTATAGATGACCCTTCGC	

150-ml glass bottles with a 50-ml working volume in MTC defined medium on 5 g/liter (14.4 mM or 0.72 mmol) cellobiose, as previously described (11), with the following modifications for *T. saccharolyticum*: urea was replaced with ammonium chloride, and thiamine hydrochloride was added to a final concentration of 4 mg/liter. Growth medium for Δ pyrF strains was supplemented with 40 mg/liter uracil. For fermentation and biochemical nfnAB complementation experiments on xylose, strains were grown in 35-ml tubes on modified DSMZ M122 rich medium in 5 g/liter xylose and 4.5 g/liter yeast extract. Samples were taken during mid-log phase for biochemical assays while growth was allowed to proceed for 96 h for fermentation product quantification. All fermentation experiments were performed in triplicate.

Heterologous expression of *T. saccharolyticum* nfnAB. The putative *T. saccharolyticum* nfnAB operon was cloned into a pEXP5-NT TOPO expression vector (Life Technologies) and transformed into *E. coli* DH5 α cells (Life Technologies). Plasmids were sequenced using primers provided with the kit, and a plasmid with the correct sequence was named pJLO30. For expression, pJLO30 was transformed into *E. coli* T7 Express lysY/I^q cells (New England Biolabs), grown and induced as previously described (6), and scaled down to 150-ml bottles. Briefly, cells were grown on tryptone-phosphate broth in shaking incubators for 20 h. After 20 h, stirring was stopped, and cultures were induced with isopropyl β -D-thiogalactopyranoside (IPTG). Cysteine (0.12 g/liter), ferrous sulfate (0.1 g/liter), ferric citrate (0.1 g/liter), and ferric ammonium citrate (0.1 g/liter) were added to enhance iron-sulfur cluster synthesis. Cells were incubated for another 20 h at 27°C and then separated from the medium by centrifugation and stored anaerobically in serum vials at -80°C until used.

Preparation of cell extracts. All steps were performed in a Coy (Grass Lake, MI) anaerobic chamber to maintain anoxic conditions. Cells were lysed by a 20-min incubation in an anaerobic buffer containing 50 mM morpholinopropanesulfonic acid (MOPS) sodium salt (pH 7.5), 5 mM dithiothreitol (DTT), 1 U of Ready-Lyse lysozyme/100 μ l (Epicentre Biotechnologies, Madison, WI), and 1 U/100 μ l DNase I (Thermo Scientific, Waltham, MA). Lysed cells were centrifuged for 15 min at 12,000 \times g, the pellet was discarded, and the supernatant was kept as cell-free-extract. Protein from the resulting cell extract was measured using Bio-Rad (Hercules, CA) protein assay dye reagent, with bovine serum albumin (Thermo Scientific) as a standard.

Biochemical assays. All biochemical assays, manipulations, and polyacrylamide gel electrophoresis (PAGE) were performed in a Coy anaerobic chamber with an atmosphere of 85% N₂, 10% CO₂, and 5% H₂ at

55°C. Oxygen was maintained at <5 ppm by use of a palladium catalyst. Solutions used were allowed to exchange gas in the anaerobic chamber for at least 48 h prior to use.

TTC reduction with NADPH (NFN activity). Assaying cell extract for NFN activity using triphenyltetrazolium chloride (TTC) was based on the method of Wang et al. (6), modified for use in a 96-well plate. Changes in absorbance were measured in a Powerwave XS plate reader (Biotek, Winooski, VT) at 55°C as previously described (11). The assay mixture contained 50 mM MOPS sodium salt (pH 7.5), 10 mM β -mercaptoethanol, 12 μ M flavin adenine dinucleotide (FAD), 0.5 mM NADP⁺, 40 mM glucose-6-phosphate, 0.2 U of glucose-6-phosphate dehydrogenase (Af-fymetrix, Santa Clara, CA), 0.4 mM TTC, and 2 mM NAD⁺ as needed. Cell extract was combined with 200 μ l of reaction mixture with and without NAD⁺. TTC reduction was monitored for 15 min at 546 nm ($\epsilon = 9.1 \text{ mM}^{-1} \text{ cm}^{-1}$).

Benzyl viologen reduction with NADPH on native PAGE (FNOR activity). Separating proteins anaerobically using native PAGE was based on the method of Fournier et al. (12) with minor modifications. Twenty minutes prior to loading cell extract, 20 μ l of 2 mM sodium dithionite (DT) was loaded into each well of a 4 to 20% nondenaturing polyacrylamide gel (Bio-Rad). Cell extract containing approximately 0.1 mg of protein was then loaded into the gel using 5 \times native loading buffer containing 62.5 mM Tris-HCl (pH 6.8), 40% glycerol, and 0.01% bromophenol blue. The gel was run at 200 V for 80 min in running buffer containing 25 mM Tris-HCl (pH 8.5) and 192 mM glycine. After electrophoresis, the gel was placed in prewarmed 55°C enzyme assay buffer containing 50 mM MOPS (pH 7.5) and 8 mM benzyl viologen (BV). DT was added until the solution reached an OD at 578 nm of 0.01 to 0.1. The reaction was started with the addition of 1.5 mM NADPH, and the mixture was incubated for 15 min. Bands of reduced BV were fixed by adding 24 mM TTC.

Benzyl viologen:NAD(P)H oxidoreductase activity of cell extracts (FNOR activity). Benzyl viologen:NAD(P)H oxidoreductase activity was measured as previously described (4) with minor modifications using the following conditions: 50 mM MOPS (pH 7.5), 0.5 mM DTT, 1 mM BV, and 0.2 mM NAD(P)H. DT was added until the solution reached an OD at 578 nm of 0.01 to 0.1 ($\epsilon = 7.8 \text{ mM}^{-1} \text{ cm}^{-1}$). Changes in absorbance were measured with an 8453 UV-visible light (UV-Vis) spectrophotometer (Agilent Technologies, Santa Clara, CA).

Alcohol and aldehyde dehydrogenase activity of cell extracts. Alcohol dehydrogenase (ADH) and aldehyde dehydrogenase (ALDH) activities were measured as previously described (5). ADH and ALDH were

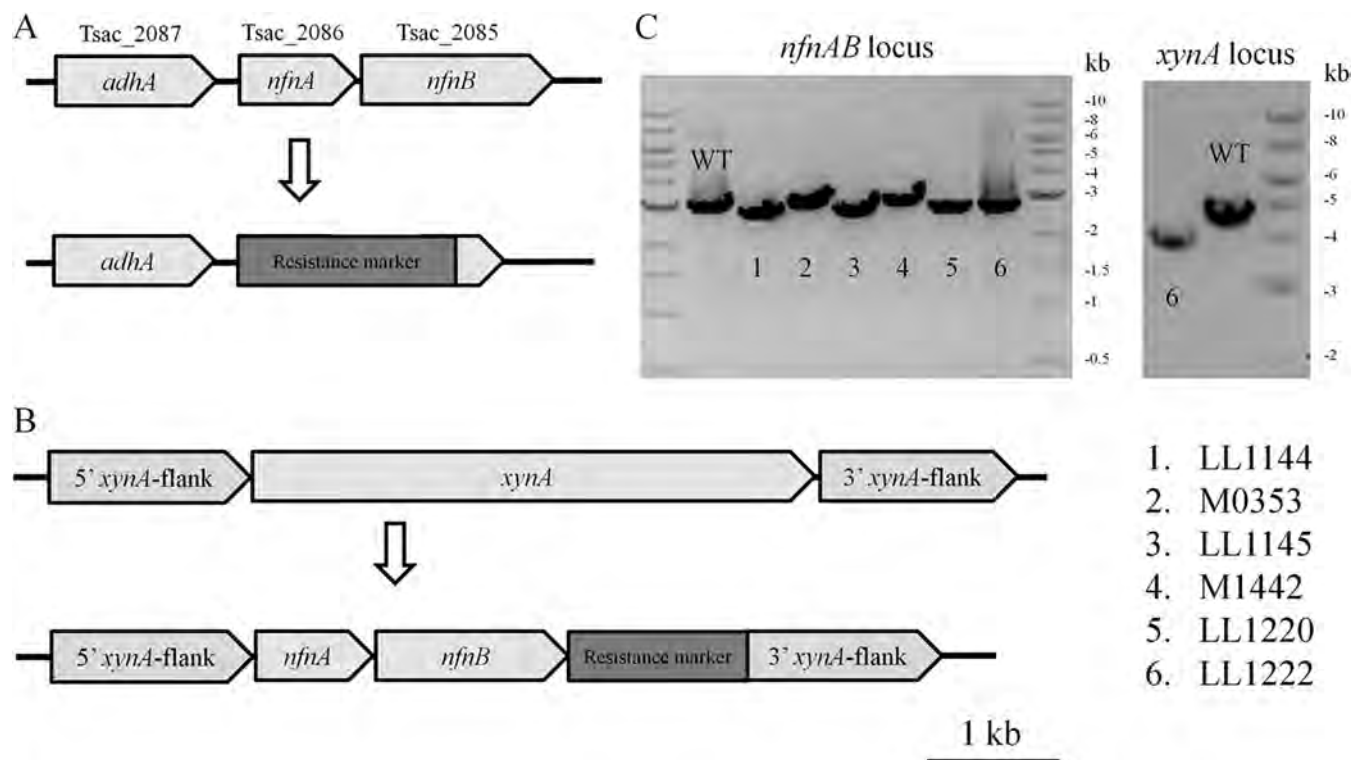


FIG 1 PCR confirmation of genetic manipulations of *nfnAB* in *T. saccharolyticum*. (A) Schematic for deletion of *nfnAB* in *T. saccharolyticum* strains. (B) Schematic for insertion of *nfnAB* under the control of the *xynA* promoter. (C) PCR analysis of *T. saccharolyticum* strains JW/SL-YS485 (WT), M0353 ($\Delta pta \Delta ack \Delta ldh \Delta pyrF$), and M1442 ($\Delta pta \Delta ack \Delta ldh \Delta adhE^{G544D}$) show the expected 3.1-kb external fragment length of *nfnAB*. Strains LL1144 ($\Delta nfnAB::Kan^r$), LL1145 ($\Delta pta \Delta ack \Delta ldh \Delta pyrF \Delta nfnAB::Kan^r$), LL1220 (M1442 $\Delta nfnAB::Kan^r$), and LL1222 (LL1220 $\Delta xynA::nfnAB$ Ery^r) with a disrupted *nfnAB* show a smaller 2.9-kb *nfnAB* locus fragment (left panel). The *xynA* locus of LL1222 compared with that of JW/SL-YS485 (WT) shows the successful integration of *nfnAB* under the control of the *xynA* promoter, which results in a reduction in fragment size from 4.7 kb to 4 kb (right panel). The DNA marker is a 1-kb ladder from New England Biolabs.

monitored by measuring NAD(P)H oxidation at 340 nm ($\epsilon = 6,220 \text{ M}^{-1} \text{ cm}^{-1}$). For ADH measurements, the reaction mixture contained 100 mM Tris-HCl buffer (pH 7.0), 5 μM FeSO_4 , 0.25 mM NAD(P)H, 18 mM acetaldehyde, and 1 mM DTT. For ALDH measurements, the reaction mixture contained 100 mM Tris-HCl buffer (pH 7.0), 5 μM FeSO_4 , 0.25 mM NAD(P)H, 1.25 mM acetyl-CoA, 1 mM DTT, and 2 mM 2,3-dimethoxy-5-methyl-*p*-benzoquinone.

Glucose-6-phosphate dehydrogenase and isocitrate dehydrogenase activity of cell extracts. Glucose-6-phosphate dehydrogenase (13) and isocitrate dehydrogenase (14) activities were measured as previously described following the reduction of NADP^+ at 340 nm. For glucose-6-phosphate dehydrogenase measurements, the reaction mixture contained 100 mM Tris-HCl buffer (pH 7.5), 2.5 mM MnCl_2 , 6 mM MgCl_2 , 2 mM glucose-6-phosphate, 1 mM DTT, and 1 mM NADP^+ . For isocitrate dehydrogenase activity, the reaction mixture contained 25 mM MOPS (pH 7.5), 5 mM MgCl_2 , 2.5 mM MnCl_2 , 100 mM NaCl, 1 mM DTT, 1 mM DL-isocitrate, and 1 mM NADP^+ .

Analytical techniques. Fermentation products in the liquid phase (cellobiose, xylose, ethanol, lactate, acetate, and formate) were measured using a Waters (Milford, MA) high-performance liquid chromatograph (HPLC) with an HPX-87H column as previously described (11). H_2 was determined by measuring total pressure and the H_2 percentage in the headspace. The headspace gas pressure in bottles was measured using a digital pressure gauge (Ashcroft, Stratford, CT). The headspace H_2 percentage was measured using a gas chromatograph (model 310; SRI Instruments, Torrance, CA) with a HayeSep D packed column using a thermal conductivity detector with nitrogen carrier gas. Pellet carbon and nitrogen, used as a measurement of cell mass (15), were measured with a Shi-

mazu TOC-V CPH elemental analyzer with TNM-1 and ASI-V modules (Shimadzu Corp., Columbia, MD) as previously described (16).

RESULTS

Genetic manipulation of *nfnAB*. To determine the role of *nfnAB* in metabolism, *nfnAB* was deleted in the following *T. saccharolyticum* strains: wild-type (WT) JW/SL-YS485, M0353 (17), and M1442 (18). The resulting $\Delta nfnAB::Kan^r$ strains were LL1144, LL1145, and LL1220, respectively (Table 1). M0353 and M1442 are strains that had previously been engineered for improved ethanol yield. In strain LL1220 (M1442 $\Delta nfnAB$), the *nfnAB* deletion was complemented with *nfnAB* under the control of the *xynA* promoter to generate strain LL1222. The *xynA* promoter allows *nfnAB* to be conditionally expressed in the presence of xylose (19). Strategies for manipulation of *nfnAB* and PCR gels confirming *nfnAB* genetic modifications in *T. saccharolyticum* are shown in Fig. 1.

NAD^+ -stimulated TTC reduction with NADPH in cell extracts (NFN activity). To confirm NFN activity and biochemical changes associated with *nfnAB* deletion, we measured NAD^+ -stimulated reduction of TTC with NADPH in cell extracts of *T. saccharolyticum* (Table 3). Increased TTC reduction in the presence of NAD^+ is characteristic of NFN activity (6). Cell extracts of *T. saccharolyticum* strain JW/SL-YS485 (wild type for *nfnAB*) showed NAD^+ -stimulated reduction of TTC with NADPH,

TABLE 3 Specific activities of NfnAB from *T. saccharolyticum*

Strain	NADPH → TTC		NfnAB activity
	NAD ⁺ condition ^a	Sp act (μmol/min/mg protein) ^b	
JW/SL-YS485 (WT)	–	0.34 (0.10)	2-fold stimulation
	+	0.69 (0.15)	
LL1144 ($\Delta nfnAB::Kan^+$)	–	0.20 (0.08)	None
	+	0.13 (0.10)	

^a The presence (+) and absence (–) of NAD⁺ are indicated.

^b Values in parentheses are standard deviations.

which disappeared in strain LL1144 (JW/SL-YS485 $\Delta nfnAB$). This confirms that NFN activity is encoded by Tsac_2085-Tsac_2086.

Alternative NADPH-generating reactions. With the loss of NFN activity, a potential source of NADPH in *T. saccharolyticum*, we wondered how NADPH was generated for biosynthetic reactions. We tested for the presence of a functional oxidative pentose phosphate pathway in JW/SL-YS485 by assaying for glucose-6-phosphate dehydrogenase and found significant activity (0.35 U/mg protein). We also found significant NADPH-linked isocitrate dehydrogenase activity (0.67 U/mg protein), another NADPH-generating reaction.

Native PAGE assay (FNOR activity). Since cell extracts contain multiple redox-active enzymes, we explored ways to determine the NfnAB activity of specific proteins within the cell extract. Native PAGE has been used to assay hydrogenase activity with redox-sensitive viologen and TTC dyes (12). We applied this principle to identify the presence of NfnAB, since the NfnAB complex from *C. kluyveri* was shown to strongly catalyze BV reduction with NADPH (6). Cell extracts of *T. saccharolyticum* JW/SL-YS485 (wild type for *nfnAB*) and LL1144 (JW/SL-YS485 $\Delta nfnAB$) and of *E. coli* heterologously expressing *T. saccharolyticum nfnAB* were separated by PAGE in an anaerobic chamber. The PAGE gel was then incubated in prewarmed enzyme activity buffer containing NADPH and BV. Bands indicating BV reduction, consistent with the presence or absence of *nfnAB*, were identified in both the *T. saccharolyticum* and *E. coli nfnAB* expression strains (Fig. 2, arrow). The bands in the upper portion of the gel in *T. saccharolyticum* appeared before NADPH was added to the buffer and are suspected to be hydrogenases.

Alcohol dehydrogenase, aldehyde dehydrogenase, and ferredoxin:NAD(P)H oxidoreductase (FNOR) activity of cell extracts. Cell extracts were assayed for ADH, ALDH, and FNOR activity (Table 4). The presence of *nfnAB* genes corresponds to high NADPH-linked BV activity in all tested strains, while deletion of *nfnAB* genes corresponds to low NADPH-linked BV activity (<0.07), showing that *nfnAB* is responsible for most of the NADPH-linked BV reduction in *T. saccharolyticum*.

Interestingly, NADH-linked BV activity remained high in all strains regardless of whether *nfnAB* was present, suggesting that it is not the sole FNOR in *T. saccharolyticum*. ADH and ALDH activities were primarily NADH linked in strains JW/SL-YS485 (wild type for *nfnAB*), LL1144 (JW/SL-YS485 $\Delta nfnAB$), and M0353 ($\Delta pta \Delta ack \Delta ldh \Delta pyrF$) and almost exclusively NADH linked in LL1145 (M0353 $\Delta nfnAB$). In contrast, M1442 ($\Delta pta \Delta ack \Delta ldh adhE^{G544D}$) (where *adhE*^{G544D} is the G-to-D change at position

544 encoded by *adhE*) and LL1220 (M1442 $\Delta nfnAB$) have primarily NADPH-linked ADH and ALDH activities.

Fermentation products of deletion strains. After biochemical characterization of activities from cell extracts, the effect of *nfnAB* deletions on fermentation product distribution was measured (Table 5). Deletion of *nfnAB* in the wild-type strain (resulting in strain LL1144) had little effect on fermentation products, with the exception of H₂ (46% increase) and acetate (21% increase) and of cell mass (25% decrease), measured by pellet carbon and nitrogen. Deletion of *nfnAB* in the M0353 ($\Delta pta \Delta ack \Delta ldh \Delta pyrF$) ethanologen strain (resulting in strain LL1145) had no substantial effect on fermentation products.

Deletion of *nfnAB* in the M1442 ($\Delta pta \Delta ack \Delta ldh adhE^{G544D}$) ethanologen strain (resulting in strain LL1220), however, gave different results. Ethanol yield, which had been about 80% of the theoretical value in M1442, was reduced to about 30% of theoretical in LL1220. H₂ production increased 10-fold, to near JW/SL-YS485 levels, and biomass, measured by pellet carbon and nitrogen, was reduced by about half. Succinate, which was not previously detected as a significant fermentation product, was present in the medium. Despite detection of this new fermentation product, carbon and electron recoveries were poor, resulting in a 50% recovery of each.

Complementation of *nfnAB* in strain LL1220. The role of *nfnAB* in ethanol production was further confirmed by a complementation experiment at the *xynA* locus. This locus had previously been used for xylose-inducible expression of genes (19). The *xynA* gene was replaced with *nfnAB* under the control of the *xynA* promoter in strain LL1220 (M1442 $\Delta nfnAB$) to make strain LL1222 (LL1220 $\Delta xynA::nfnAB$ Ery^r) (Fig. 1B). We grew strains M1442, LL1220, and LL1222 in M122 medium with 5 g/liter xylose (both as a carbon source and to induce expression of *nfnAB*) and tested for ethanol formation and NADPH:BV reduction (Table 6). We found significant NADPH:BV activity in M1442.

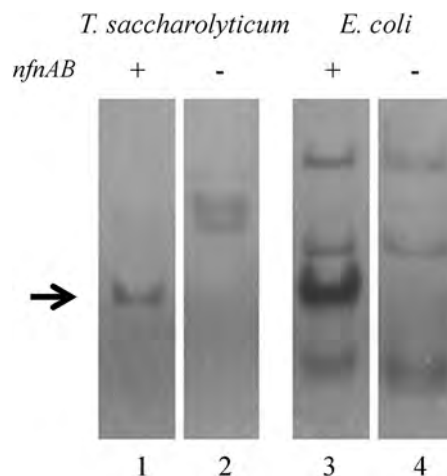


FIG 2 Native PAGE analysis for NfnAB activity. Cell extracts were run simultaneously on PAGE gels for 80 min and then incubated in an assay solution consisting of benzyl viologen (BV). NADPH was added to start the reaction. A band of BV reduction corresponding with NfnAB activity was then fixed in the gel with triphenyltetrazolium chloride, marked by the arrow. Lane 1, *T. saccharolyticum* cell extract of JW/SL-YS485; lane 2, *T. saccharolyticum* cell extract of LL1144; lane 3, *E. coli* cell extract with pJLO30 expressing *nfnAB*; lane 4, extract of *E. coli* with no plasmid. Relevant genotypes are indicated above the gels.

TABLE 4 Alcohol/aldehyde/benzyl viologen NAD(P)H activities in cell extracts

Enzyme	Activity ^a (U/mg protein) (SD) by strain					
	JW/SL-YS485 (WT)	LL1144 ($\Delta nfnAB$)	M0353 ($\Delta pyrF \Delta pta \Delta ack \Delta ldh$)	LL1145 (M0353 $\Delta nfnAB::Kan^r$)	M1442 ($\Delta pta \Delta ack \Delta ldh adhE^{G544D}$)	LL1220 (M1442 $\Delta nfnAB::Kan^r$)
NADH-ADH	7.06 (0.50)	7.05 (1.73)	0.47 (0.11)	12.40 (0.85)	0.18 (0.14)	0.00 (0.02)
NADPH-ADH	0.95 (0.58)	0.19 (0.02)	0.42 (0.05)	0.00 (0.02)	1.10 (0.42)	0.42 (0.10)
NADH-ALDH	0.41 (0.13)	0.33 (0.11)	1.32 (0.31)	0.21 (0.03)	0.09 (0.02)	0.00 (0.16)
NADPH-ALDH	0.05 (0.04)	0.00 (0.12)	0.08 (0.08)	0.04 (0.02)	0.50 (0.05)	0.41 (0.06)
NADH-BV	0.33 (0.05)	0.33 (0.05)	0.53 (0.24)	0.21 (0.04)	0.20 (0.03)	0.48 (0.01)
NADPH-BV	0.18 (0.03)	0.04 (0.03)	0.48 (0.28)	0.04 (0.01)	0.53 (0.23)	0.06 (0.01)

^a Values are averages from triplicate experiments.

Deletion of *nfnAB* eliminated most of the NADPH:BV activity (strain LL1220). Expression of *nfnAB* with the *xynA* promoter restored NADPH:BV activity (strain LL1222) although only to about half of the wild-type level.

Next, we looked at the ethanol formation of M1442, LL1220, and LL1222. We found that both M1442 and LL1222 had high yields of ethanol from consumed xylose (109% and 69%, respectively), while LL1220 had a much lower yield of ethanol (19%), suggesting that *nfnAB* was important to ethanol formation in M1442. Xylose consumption was impacted in both mutant strains LL1220 and LL1222 as the strains were unable to consume the provided xylose within 96 h although strain LL1222 consumed more xylose than strain LL1220.

DISCUSSION

In this work, we set out to understand the physiological role of *nfnAB* in *T. saccharolyticum* and several mutants engineered for increased ethanol production. In the wild-type strain, we were able to show NAD⁺-stimulated TTC reduction with NADPH, a reaction indicative of its function as a bifurcating enzyme. We demonstrated a new assay for detecting the NfnAB complex using a native-PAGE-based assay, which we confirmed by deletion in *T. saccharolyticum* and heterologous expression in *E. coli*, thus linking the coding region annotated as Tsac_2085-Tsac_2086 with this activity. Furthermore, this activity is necessary for high-yield ethanol production in one ethanologen strain of *T. saccharolyticum* (M1442) but not in another similar strain (M0353).

What causes the different responses to loss of *nfnAB* in the

different strains of *T. saccharolyticum* engineered for ethanol formation? A possible answer is that one strain uses primarily NADPH for ethanol production, while the other uses primarily NADH. We think that strain M1442 uses the NADPH-linked pathway, based on enzyme assay data from Table 4. We also think that a previously described *T. saccharolyticum* ethanologen strain, ALK2, also uses this pathway. In strain ALK2, an NADPH preference was seen for ADH, ALDH, and BV reductase activities in cell extract (3). Unfortunately, genetic manipulation of *nfnAB* was impossible in ALK2, as ALK2 already has the Kan and Erm resistance markers, which are the only two antibiotic resistance genes available for *T. saccharolyticum*. Both ALK2 and M1442 contain mutations in *adhE* that have been shown to change the cofactor specificity of AdhE from primarily NADH linked to NADPH linked (20).

In contrast, the wild-type, LL1144, and LL1145 strains appear to use the NADH-linked ethanol production pathway. These strains use NADH for ADH, ALDH, and BV reductase activities in cell extracts (Table 4). Furthermore, none of these strains have mutations in their *adhE* genes. Based on enzyme assay data, strain M0353 may be able to use both the NADH- and NADPH-linked ethanol production pathways. NfnAB appears to function in a primarily biosynthetic role in the wild-type strain as the $\Delta nfnAB$ LL1144 strain had less biomass than its wild-type parent. This is despite LL1144 having more acetate/ATP formation (acetate production results in ATP formation [4]).

Why does strain LL1220 (M1442 $\Delta nfnAB$) have trouble growing and making ethanol? Since NADPH is the main cofactor used

TABLE 5 Fermentation products of *T. saccharolyticum*

Strain	Yield (mmol) of ^a :									Calculated CDW (mg) ^b	O/R index ^c
	Cellobiose	Lactate	Ethanol	Acetate	H ₂	Formate	Succinate	Pellet C	Pellet N		
JW/SL-YS485 (WT)	0.02 (0.04)	0.14 (0.03)	1.26 (0.02) [44]	0.76 (0.05)	1.84 (0.19)	0.02 (0.02)	0.00 (0.00)	1.01 (0.03)	0.26 (0.04)	28.12	0.9
LL1144 ($\Delta nfnAB$)	0.00 (0.00)	0.07 (0.03)	1.31 (0.09) [45]	0.92 (0.06)	2.69 (0.09)	0.04 (0.03)	0.00 (0.00)	0.76 (0.14)	0.19 (0.03)	21.16	1
M0353 ($\Delta pyrF \Delta pta \Delta ack \Delta ldh$)	0.00 (0.00)	0.02 (0.00)	2.19 (0.38) [76]	0.05 (0.02)	0.30 (0.18)	0.27 (0.02)	0.00 (0.00)	0.80 (0.24)	0.20 (0.06)	22.27	0.9
LL1145 (M0353 $\Delta nfnAB::Kan^r$)	0.00 (0.00)	0.03 (0.01)	2.41 (0.11) [83]	0.06 (0.06)	0.34 (0.17)	0.24 (0.05)	0.00 (0.00)	0.76 (0.24)	0.20 (0.06)	21.16	1
M1442 ($\Delta pta \Delta ack \Delta ldh adhE^{G544D}$)	0.00 (0.00)	0.00 (0.00)	2.43 (0.13) [84]	0.07 (0.03)	0.16 (0.00)	0.21 (0.01)	0.00 (0.00)	0.74 (0.07)	0.25 (0.05)	20.6	1
LL1220 (M1442 $\Delta nfnAB::Kan^r$)	0.05 (0.01)	0.00 (0.00)	0.76 (0.05) [28]	0.02 (0.00)	1.60 (0.00)	0.26 (0.01)	0.09 (0.01)	0.32 (0.02)	0.09 (0.01)	8.91	0.5

^a For quantification of fermentation products, strains were used at a working volume of 50 ml on 0.72 mmol cellobiose. Values are averages from triplicate experiments, and standard deviations are given in parentheses. For ethanol yield, the percentage relative to the theoretical yield is given in brackets.

^b CDW, cell dry weight calculated from pellet carbon (5, 15).

^c O/R, oxidation/reduction.

TABLE 6 Ethanol formation and NADPH:BV reduction in *T. saccharolyticum*^a

Strain	Xylose consumed (mmol)	Ethanol (mmol)	Ethanol yield from consumed xylose (%)	NADPH-BV activity (U/mg cell extract)
M1442 (Δ <i>pta</i> Δ <i>ack</i> Δ <i>ldh</i> <i>adhE</i> ^{G544D})	1.17 (0.00)	2.12 (0.05)	109	0.41 (0.07)
LL1220 (M1442 Δ <i>nfnAB</i> ::Kan ^r)	0.48 (0.23)	0.15 (0.10)	19	0.05 (0.01)
LL1222 (LL11220 <i>xyxA</i> :: <i>nfnAB</i> -Erm ^r)	0.81 (0.04)	0.93 (0.35)	69	0.18 (0.05)

^a Strains were used at a working volume of 35 ml on 1.17 mmol (5 g/liter) xylose. Values are averages from triplicate experiments, and standard deviations are given in parentheses.

for ethanol production in the M1442 lineage, without *nfnAB*, the LL1220 strain may have trouble balancing electron metabolism, in particular NAD(P)H cofactors and ferredoxin reoxidation. As NFN activity oxidizes NADH and ferredoxin and reduces NADP⁺, it sits at a central junction in electron metabolism. In strain LL1220, loss of ferredoxin oxidation by the NfnAB complex seems to cause significant H₂ formation. Significant H₂ formation from reduced ferredoxin is incompatible with high ethanol yield (reactions 1 and 2) (21) and suggests that electron metabolism is imbalanced in this strain. High H₂ formation, presumably from reduced ferredoxin (10), also implies significant acetyl-CoA formation through pyruvate:ferredoxin oxidoreductase (PFOR) and may point to the source of missing fermentation products. Succinate was detected as a fermentation product in this strain, suggestive of functional tricarboxylic acid (TCA) cycle enzymes that may play a role in metabolism in this strain. However, carbon and electron recoveries were poor in this strain, and their definitive fate remains a mystery.

Although mutations in *adhE* have been shown to produce NADPH-linked ADH activity (20, 22, 23), another possible source of NADPH-linked ADH activity is the *adhA* gene, Tsac_2087. It has been shown that in a *T. saccharolyticum* *adhE* deletion strain, there were still significant levels of NADPH-linked ADH activity, suggesting that there may be other functional NADPH-linked alcohol dehydrogenases (5). Interestingly, this predicted NADPH-linked alcohol dehydrogenase, *adhA*, is located directly upstream of *nfnAB* (Fig. 1A). There is evidence that *adhA* is expressed at very high levels, at least in wild-type *T. saccharolyticum*. A transcriptomic study of this strain found *adhA* to be consistently among the highest 50 genes expressed (24). The close proximity of these genes suggests a shared biological function and perhaps coregulation. This gene configuration is shared among the closely related *Thermoanaerobacter* and *Thermoanaerobacterium* species (25) previously investigated for ethanol formation, for example, *Thermoanaerobacter mathranii*, *Thermoanaerobacter pseudethanolicus*,

and *Thermoanaerobacter brockii* (Table 7). Many of these bacteria have demonstrated high ethanol yields (13, 26, 27). Interestingly, many *Thermoanaerobacter* species also carry a predicted *adhB* gene nearby as well, which encodes a Zn-dependent bifunctional alcohol/aldehyde dehydrogenase that uses NADPH instead of NADH as a cofactor (28–30) and is believed to be important for ethanol formation in *T. pseudethanolicus* (28, 31). In a proteomic study of *T. pseudethanolicus*, the products of *nfnAB*, *adhA*, and *adhB* were among the top 50 proteins detected (32). In this study, these proteins were significantly downregulated in response to furan aldehyde addition and coincided with reduced ethanol yields, which may be due partially to downregulation of these proteins.

There is previous evidence for NADPH as the primary cofactor utilized for ethanol formation. In a *T. pseudethanolicus* strain engineered for ethanol tolerance, it was noted that NADH-linked ADH, ALDH, and FNOR activities were lost, while NADPH-linked activities remained (33). While this strain produced less ethanol than the parent strain, the ethanol-tolerant strain still produced high yields of ethanol (34). Additionally, it was shown that *T. brockii* had mostly NADPH-linked ADH activity (13). A meta-analysis of metabolic pathways in select fermentative microorganisms noted that all major ethanol formers included *adhE* except one (21). The exception was *Caldanaerobacter subterraneus* subsp. *tengcongensis* (formerly *Thermoanaerobacter tengcongensis* MB4), which the authors noted encoded only alcohol dehydrogenases and lacked aldehyde dehydrogenases yet was reported to produce significant amounts of ethanol. The locus containing *nfnAB* and predicted aldehyde and alcohol dehydrogenases may explain ethanol formation in *C. subterraneus* subsp. *tengcongensis*. One of the alcohol dehydrogenase genes, TTE0695, is a predicted *adhB* gene, which shares high similarity (>95% identity) to *adhB* from *T. mathranii* and *T. pseudethanolicus*. AdhB can catalyze the NADPH-dependent conversion of acetyl-CoA to ethanol (reaction 3) (28) and could be the source of ethanol formation in *C. subterraneus* subsp. *tengcongensis*. Both the ALDH and ADH reac-

TABLE 7 Comparison of selected genes encoding NfnAB and various alcohol dehydrogenases

Organism	Homolog (% identity) ^a of:				
	<i>adhE</i>	<i>adhB</i>	<i>adhA</i>	<i>nfnA</i>	<i>nfnB</i>
<i>Thermoanaerobacterium saccharolyticum</i>	Tsac_0416 (100)	NF	Tsac_2087 (100)	Tsac_2086 (100)	Tsac_2085 (100)
<i>Thermoanaerobacterium thermosaccharolyticum</i>	Tthe_2646 (97)	NF	Tthe_1156 (93)	Tthe_1157 (91)	Tthe_1158 (91)
<i>Thermoanaerobacter pseudethanolicus</i> 39E	Teth39_0206 (86)	Teth39_0218 (100)	Teth39_0220 (86)	Teth39_0217 (64)	Teth39_0216 (73)
<i>Thermoanaerobacterium</i> sp. strain X514	Teth514_0627 (86)	Teth514_0653 (98)	Teth514_0654 (88)	Teth514_0652 (65)	Teth514_0651 (73)
<i>Thermoanaerobacter mathranii</i>	Tmath_2110 (85)	Tmath_2094 (97)	Tmath_2093 (86)	Tmath_2095 (64)	Tmath_2096 (73)
<i>Thermoanaerobacter brockii</i>	Thebr_0212 (86)	Thebr_0224 (100)	Thebr_0226 (86)	Thebr_0223 (64)	Thebr_0222 (73)
<i>Caldanaerobacter subterraneus</i> subsp. <i>tengcongensis</i>	NF	TTE0695 (98)	TTE0696 (86)	TTE0694 (64)	TTE0693 (72)
<i>Thermoanaerobacter kivui</i>	NF	TKV_c22260 (97)	NF	TKV_c22270 (64)	TKV_c22280 (73)

^a Percent amino acid identity for the encoded protein was determined relative to the *T. saccharolyticum* reference for all genes except *adhB*, for which the reference was *T. pseudethanolicus* 39E. NF, not found.

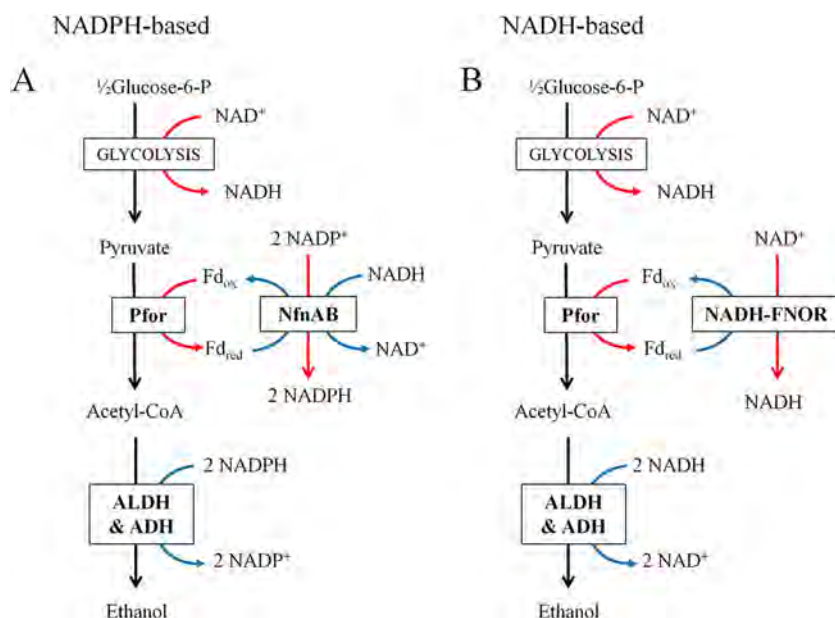


FIG 3 Proposed electron-based models for stoichiometric ethanol production in *T. saccharolyticum* based on NADPH and NADH. (A) NADPH-based ethanol formation relies on the electron transfer from NADH (generated from glyceraldehyde-3-phosphate dehydrogenase) and reduced ferredoxin to 2NADP^+ , catalyzed by the NfnAB complex. The 2 NADPH molecules are then consumed by NADPH-dependent aldehyde and alcohol dehydrogenase activity. (B) NADH-based ethanol formation relies on a yet uncharacterized ferredoxin: NAD^+ oxidoreductase (NADH-FNOR) to transfer electrons from reduced ferredoxin to NAD^+ . The NADH generated by glyceraldehyde-3-phosphate dehydrogenase and NADH-FNOR is then consumed by NADH-dependent aldehyde and alcohol dehydrogenase activity. Red arrows indicate that cofactor is reduced, while blue arrows indicate that cofactor is oxidized. Pfor, pyruvate:ferredoxin oxidoreductase; ALDH, aldehyde dehydrogenase; ADH, alcohol dehydrogenase; FNOR, ferredoxin: NADH oxidoreductase; Fd, ferredoxin.

tions in *C. subterraneus* subsp. *tengcongensis* were shown to be NADPH linked (35) and could possibly be catalyzed by AdhB and/or AdhA.

How does *T. saccharolyticum* make ethanol at high yield? If pyruvate:ferredoxin oxidoreductase (PFOR) is the enzyme responsible for pyruvate oxidation as believed (4), then there must be electron transfer from reduced ferredoxin to NAD(P)^+ . We have shown that the NfnAB complex can play a role in that electron transfer. However, it appears that there may be other unidentified FNOR-like enzymes responsible for the transfer of electrons from reduced ferredoxin to NAD^+ . NfnAB does not strongly reduce benzyl viologen with NADH (6), yet substantial NADH:BV reductase activities were previously seen in cell extracts (3, 4). Indeed, in cell extracts lacking *nfnAB*, we measured high levels of NADH:BV reductase activity, suggesting that there may be other enzymes with FNOR activity. Thus, we propose two different mechanisms for stoichiometric yield of ethanol in *T. saccharolyticum*, one based on NADPH and NfnAB and the other based on NADH and a yet undescribed NADH-FNOR (Fig. 3). This undescribed NADH-FNOR activity could be provided by the Rnf complex (7), but we could not identify genes corresponding to known Rnf complexes. Much is still unknown about the enzymes involved in the metabolism of anaerobic thermophiles, especially in the context of their importance in end product formation.

We also demonstrated the presence of two other NADPH-generating reactions, glucose-6-phosphate dehydrogenase and NADP^+ -linked isocitrate dehydrogenase, which are possibly indicative of an oxidative pentose phosphate pathway and a tricarboxylic acid cycle, respectively. It was previously shown by ^{13}C labeling in *Thermoanaerobacter* that utilization of the oxidative pentose phosphate pathway varied by both species and the sugar

utilized (36). In this study, *Thermoanaerobacter* sp. strain X514 was shown to have minimal flux through the oxidative pentose phosphate pathway, and it was proposed that Teth514_0652 provided NADPH for biosynthesis, which has a high degree of identity to NfnA from *T. saccharolyticum* (Table 7). A bifurcated TCA cycle has been previously demonstrated in *Clostridium acetobutylicum* as having a role in biosynthetic reactions (37), and this feature may be present in *T. saccharolyticum* as well. These reactions may be responsible for the limited ethanol production observed when *nfnAB* was deleted from strain M1442, although additional work will be necessary for definitive confirmation.

In conclusion, we report the first published deletion of *nfnAB* and characterize its role in *T. saccharolyticum* metabolism. We describe a new native-gel-based assay for detection of NfnAB. We describe biochemical and fermentation product changes resulting from the genetic manipulation of *nfnAB* and show that *nfnAB* is important for ethanol formation at high yield in strain M1442. While NfnAB can be important for ethanol formation, we find that it is not always essential, and we provide evidence of a different NADH-linked (instead of NADPH-linked) ethanol production pathway in strain LL1145, which involves an NADH-linked FNOR (which has not yet been linked to a specific gene). Finally, we show that glucose-6-phosphate dehydrogenase and isocitrate dehydrogenase are other potential sources of NADPH generation. Although *T. saccharolyticum* was successfully engineered for high ethanol formation by inactivating acetate and lactate production, the identity, function, and interaction of enzymes involved in ethanol formation are poorly understood. NfnAB is believed to be distributed among a wide variety of microbes with diverse energy metabolisms, but its function and importance in these microbes remain largely unknown (6, 7). Elucidating these pathways is an

important part in understanding the metabolism and physiology of anaerobic microorganisms.

ACKNOWLEDGMENTS

The BioEnergy Science Center is a U.S. Department of Energy (DOE) Bioenergy Research Center supported by the Office of Biological and Environmental Research in the DOE Office of Science. This paper was authored by Dartmouth College under subcontract number 4000115284 and contract number DE-AC05-00OR22725 with the U.S. Department of Energy.

We thank the Mascoma Corporation for *T. saccharolyticum* strains. We thank Hans van Dijken for useful comments.

REFERENCES

- Wyman CE. 2007. What is (and is not) vital to advancing cellulosic ethanol. *Trends Biotechnol* 25:153–157. <http://dx.doi.org/10.1016/j.tibtech.2007.02.009>.
- Olson DG, McBride JE, Shaw AJ, Lynd LR. 2012. Recent progress in consolidated bioprocessing. *Curr Opin Biotechnol* 23:396–405. <http://dx.doi.org/10.1016/j.copbio.2011.11.026>.
- Shaw AJ, Podkaminer KK, Desai SG, Bardsley JS, Rogers SR, Thorne PG, Hogsett DA, Lynd LR. 2008. Metabolic engineering of a thermophilic bacterium to produce ethanol at high yield. *Proc Natl Acad Sci U S A* 105:13769–13774. <http://dx.doi.org/10.1073/pnas.0801266105>.
- Shaw JA, Jenney FE, Jr, Adams MWW, Lynd LR. 2008. End-product pathways in the xylose fermenting bacterium, *Thermoanaerobacterium saccharolyticum*. *Enzyme Microb Technol* 42:453–458. <http://dx.doi.org/10.1016/j.enzmictec.2008.01.005>.
- Lo J, Zheng T, Hon S, Olson DG, Lynd LR. 2015. The bifunctional alcohol and aldehyde dehydrogenase gene, *adhE*, is necessary for ethanol production in *Clostridium thermocellum* and *Thermoanaerobacterium saccharolyticum*. *J Bacteriol* 197:1386–1393. <http://dx.doi.org/10.1128/JB.02450-14>.
- Wang S, Huang H, Moll J, Thauer RK. 2010. NADP⁺ reduction with reduced ferredoxin and NADP⁺ reduction with NADH are coupled via an electron-bifurcating enzyme complex in *Clostridium kluyveri*. *J Bacteriol* 192:5115–5123. <http://dx.doi.org/10.1128/JB.00612-10>.
- Buckel W, Thauer RK. 2013. Energy conservation via electron bifurcating ferredoxin reduction and proton/Na⁺ translocating ferredoxin oxidation. *Biochim Biophys Acta* 1827:94–113. <http://dx.doi.org/10.1016/j.bbabi.2012.07.002>.
- Tripathi SA, Olson DG, Argyros DA, Miller BB, Barrett TF, Murphy DM, McCool JD, Warner AK, Rajgarhia VB, Lynd LR, Hogsett DA, Caiazza NC. 2010. Development of *pyrF*-based genetic system for targeted gene deletion in *Clostridium thermocellum* and creation of a *pta* mutant. *Appl Environ Microbiol* 76:6591–6599. <http://dx.doi.org/10.1128/AEM.01484-10>.
- Shanks RMQ, Caiazza NC, Hinsä SM, Toutain CM, O'Toole GA. 2006. *Saccharomyces cerevisiae*-based molecular tool kit for manipulation of genes from gram-negative bacteria. *Appl Environ Microbiol* 72:5027–5036. <http://dx.doi.org/10.1128/AEM.00682-06>.
- Shaw AJ, Hogsett DA, Lynd LR. 2009. Identification of the [FeFe]-hydrogenase responsible for hydrogen generation in *Thermoanaerobacterium saccharolyticum* and demonstration of increased ethanol yield via hydrogenase knockout. *J Bacteriol* 191:6457–6464. <http://dx.doi.org/10.1128/JB.00497-09>.
- Zhou J, Olson DG, Argyros DA, Deng Y, van Gulik WM, van Dijken JP, Lynd LR. 2013. Atypical glycolysis in *Clostridium thermocellum*. *Appl Environ Microbiol* 79:3000–3008. <http://dx.doi.org/10.1128/AEM.04037-12>.
- Fournier M, Dermoun Z, Durand M-C, Dolla A. 2004. A new function of the *Desulfovibrio vulgaris* Hildenborough [Fe] hydrogenase in the protection against oxidative stress. *J Biol Chem* 279:1787–1793. <http://dx.doi.org/10.1074/jbc.M307965200>.
- Lamed R, Zeikus JG. 1980. Ethanol production by thermophilic bacteria: relationship between fermentation product yields of and catabolic enzyme activities in *Clostridium thermocellum* and *Thermoanaerobium brockii*. *J Bacteriol* 144:569–578.
- Thorsness PE, Koshland DE. 1987. Inactivation of isocitrate dehydrogenase by phosphorylation is mediated by the negative charge of the phosphate. *J Biol Chem* 262:10422–10425.
- Holwerda EK, Ellis LD, Lynd LR. 2013. Development and evaluation of methods to infer biosynthesis and substrate consumption in cultures of cellulolytic microorganisms. *Biotechnol Bioeng* 110:2380–2388. <http://dx.doi.org/10.1002/bit.24915>.
- van der Veen D, Lo J, Brown SD, Johnson CM, Tschaplinski TJ, Martin M, Engle NL, van den Berg RA, Argyros AD, Caiazza NC, Guss AM, Lynd LR. 2013. Characterization of *Clostridium thermocellum* strains with disrupted fermentation end-product pathways. *J Ind Microbiol Biotechnol* 40:725–734. <http://dx.doi.org/10.1007/s10295-013-1275-5>.
- Shaw AJ, Covalla SF, Hogsett D, Herring CD. 2011. Marker removal system for *Thermoanaerobacterium saccharolyticum* and development of a markerless ethanologen. *Appl Environ Microbiol* 77:2534–2536. <http://dx.doi.org/10.1128/AEM.01731-10>.
- Lee JM, Venditti RA, Jameel H, Kenealy WR. 2011. Detoxification of woody hydrolyzates with activated carbon for bioconversion to ethanol by the thermophilic anaerobic bacterium *Thermoanaerobacterium saccharolyticum*. *Biomass Bioenergy* 35:626–636. <http://dx.doi.org/10.1016/j.biombioe.2010.10.021>.
- Currie DH, Herring CD, Guss AM, Olson DG, Hogsett DA, Lynd LR. 2013. Functional heterologous expression of an engineered full-length CipA from *Clostridium thermocellum* in *Thermoanaerobacterium saccharolyticum*. *Biotechnol Biofuels* 6:32. <http://dx.doi.org/10.1186/1754-6834-6-32>.
- Zheng T, Olson DG, Tian L, Bomble YJ, Himmel ME, Lo J, Hon S, Shaw AJ, van Dijken JP, Lynd LR. 26 May 2015. Cofactor specificity of the bifunctional alcohol and aldehyde dehydrogenase (AdhE) in wild-type and mutants of *Clostridium thermocellum* and *Thermoanaerobacterium saccharolyticum*. *J Bacteriol* <http://dx.doi.org/10.1128/JB.00232-15>.
- Carere CR, Rydzak T, Verbeke TJ, Cicek N, Levin DB, Sparling R. 2012. Linking genome content to biofuel production yields: a meta-analysis of major catabolic pathways among select H₂ and ethanol-producing bacteria. *BMC Microbiol* 12:295. <http://dx.doi.org/10.1186/1471-2180-12-295>.
- Biswas R, Zheng T, Olson DG, Lynd LR, Guss AM. 2015. Elimination of hydrogenase active site assembly blocks H₂ production and increases ethanol yield in *Clostridium thermocellum*. *Biotechnol Biofuels* 8:20. <http://dx.doi.org/10.1186/s13068-015-0204-4>.
- Brown SD, Guss AM, Karpins TV, Parks JM, Smolin N, Yang S, Land ML, Klingeman DM, Bhandiwad A, Rodriguez M, Raman B, Shao X, Mielenz JR, Smith JC, Keller M, Lynd LR. 2011. Mutant alcohol dehydrogenase leads to improved ethanol tolerance in *Clostridium thermocellum*. *Proc Natl Acad Sci U S A* 108:13752–13757. <http://dx.doi.org/10.1073/pnas.1102444108>.
- Currie DH, Guss AM, Herring CD, Giannone RJ, Johnson CM, Lankford PK, Brown SD, Hettich RL, Lynd LR. 2014. Profile of secreted hydrolases, associated proteins, and SlpA in *Thermoanaerobacterium saccharolyticum* during the degradation of hemicellulose. *Appl Environ Microbiol* 80:5001–5011. <http://dx.doi.org/10.1128/AEM.00998-14>.
- Collins MD, Lawson PA, Willems A, Cordoba JJ, Fernandez-Garayzabal J, Garcia P, Cai J, Hippe H, Farrow JA. 1994. The phylogeny of the genus *Clostridium*: proposal of five new genera and eleven new species combinations. *Int J Syst Bacteriol* 44:812–826. <http://dx.doi.org/10.1099/00207713-44-4-812>.
- Yao S, Mikkelsen MJ. 2010. Metabolic engineering to improve ethanol production in *Thermoanaerobacter mathranii*. *Appl Microbiol Biotechnol* 88:199–208. <http://dx.doi.org/10.1007/s00253-010-2703-3>.
- Wiegel J, Ljungdahl LG. 1981. *Thermoanaerobacter ethanolicus* gen. nov., spec. nov., a new, extreme thermophilic, anaerobic bacterium. *Arch Microbiol* 128:343–348. <http://dx.doi.org/10.1007/BF00405910>.
- Burdette D, Zeikus JG. 1994. Purification of acetaldehyde dehydrogenase and alcohol dehydrogenases from *Thermoanaerobacter ethanolicus* 39E and characterization of the secondary-alcohol dehydrogenase (2 degrees Adh) as a bifunctional alcohol dehydrogenase-acetyl-CoA reductive thioesterase. *Biochem J* 302:163–170.
- Yao S, Mikkelsen MJ. 2010. Identification and overexpression of a bifunctional aldehyde/alcohol dehydrogenase responsible for ethanol production in *Thermoanaerobacter mathranii*. *J Mol Microbiol Biotechnol* 19:123–133. <http://dx.doi.org/10.1159/000321498>.
- Bryant FO, Wiegel J, Ljungdahl LG. 1988. Purification and properties of primary and secondary alcohol dehydrogenases from *Thermoanaerobacter ethanolicus*. *Appl Environ Microbiol* 54:460–465.
- Pei J, Zhou Q, Jiang Y, Le Y, Li H, Shao W, Wiegel J. 2010. *Thermoanaerobacter* spp. control ethanol pathway via transcriptional regulation

- and versatility of key enzymes. *Metab Eng* 12:420–428. <http://dx.doi.org/10.1016/j.ymben.2010.06.001>.
32. Clarkson SM, Hamilton-Brehm SD, Giannone RJ, Engle NL, Tschaplinski TJ, Hettich RL, Elkins JG. 2014. A comparative multidimensional LC-MS proteomic analysis reveals mechanisms for furan aldehyde detoxification in *Thermoanaerobacter pseudethanolicus* 39E. *Biotechnol Biofuels* 7:165. <http://dx.doi.org/10.1186/s13068-014-0165-z>.
 33. Lovitt RW, Shen GJ, Zeikus JG. 1988. Ethanol production by thermophilic bacteria: biochemical basis for ethanol and hydrogen tolerance in *Clostridium thermohydrosulfuricum*. *J Bacteriol* 170:2809–2815.
 34. Lovitt RW, Longin R, Zeikus JG. 1984. Ethanol production by thermophilic bacteria: physiological comparison of solvent effects on parent and alcohol-tolerant strains of *Clostridium thermohydrosulfuricum*. *Appl Environ Microbiol* 48:171–177.
 35. Soboh B, Linder D, Hedderich R. 2004. A multisubunit membrane-bound [NiFe] hydrogenase and an NADH-dependent Fe-only hydrogenase in the fermenting bacterium *Thermoanaerobacter tengcongensis*. *Microbiology* 150:2451–2463. <http://dx.doi.org/10.1099/mic.0.27159-0>.
 36. Hemme CL, Fields MW, He Q, Deng YY, Lin L, Tu Q, Mouttaki H, Zhou A, Feng X, Zuo Z, Ramsay BD, He Z, Wu L, Van Nostrand J, Xu J, Tang YJ, Wiegel J, Phelps TJ, Zhou J. 2011. Correlation of genomic and physiological traits of *Thermoanaerobacter* species with biofuel yields. *Appl Environ Microbiol* 77:7998–8008. <http://dx.doi.org/10.1128/AEM.05677-11>.
 37. Amador-Noguez D, Feng X-J, Fan J, Roquet N, Rabitz H, Rabinowitz JD. 2010. Systems-level metabolic flux profiling elucidates a complete, bifurcated tricarboxylic acid cycle in *Clostridium acetobutylicum*. *J Bacteriol* 192:4452–4461. <http://dx.doi.org/10.1128/JB.00490-10>.